Robust Adaptive Model-Free Control of Saturated Flexible-Joint Robots Using the Bernstein-Schurer-Stancu Operator

Javad Keighobadi[1*]

Abstract: **This paper presents a new robust model-free control strategy for uncertain flexible-joint robot manipulators subject to actuator saturation and external disturbances. The proposed framework integrates a backstepping-based adaptive control architecture with the Bernstein-Schurer-Stancu (BSS) operator as a universal approximator to compensate for unknown system dynamics and uncertainties without requiring precise mathematical modeling. To circumvent the complexity explosion problem, a command-filtered control methodology with an error compensation mechanism is incorporated. Additionally, an auxiliary compensation system is developed to mitigate the adverse effects of input saturation, with its states directly utilized to construct the compensated error surfaces that drive the adaptation laws for the BSS operator coefficients. The uniform ultimate boundedness of the closed-loop system is rigorously established through recursive Lyapunov analysis. Comparative simulation studies on a flexible-joint robot manipulator demonstrate that the proposed BSS operator-based approach achieves superior tracking performance, faster convergence, and reduced computational overhead compared to a conventional fuzzy control scheme. The theoretical results validate the effectiveness of the proposed methodology for satisfactory control of flexible-joint robots under practical constraints.**

Keywords: **Model-free control, Bernstein-Schurer-Stancu operator, flexible-joint robot, Command-filtered approach, Input saturation, Stability**

I Introduction

Flexible-joint robots (FJRs) have emerged as a transformative technology in modern automation, offering compelling advantages over traditional rigid manipulators—such as lightweight construction, superior maneuverability, high load-to-weight ratios, and enhanced safety in human–robot collaborative environments [1]. These attributes render FJRs indispensable across a diverse range of application domains, from medical rehabilitation and precision assembly to space exploration and advanced manufacturing [2]. However, the inherent flexibility in the joint transmission mechanism introduces formidable control challenges, which fundamentally distinguish FJRs from their rigid counterparts.

The presence of joint flexibility doubles the number of system degrees of freedom relative to control inputs, necessitating that the link position track the actuator position through an elastic transmission element [3]. This structural characteristic, compounded by strong dynamic coupling, complex nonlinearities, and susceptibility to parameter uncertainties, renders high-precision trajectory tracking of FJRs a particularly challenging control problem [4]. In practice, FJRs are inevitably subject to various uncertainties, including unmodeled dynamics, parameter perturbations, time-varying external disturbances, and, critically, actuator saturation arising from physical limitations in torque generation [5].

[1] Shahrood University of Technology, Shahrood 36199-9516, Iran
* Corresponding Author, Email: javad.keighobadi@yahoo.com

These intertwined challenges—uncertainties, input saturation, and the higher-order complexity of flexible-joint dynamics—motivate the research presented herein. Substantial research efforts have been devoted to developing advanced control strategies for FJRs. Adaptive control schemes have been proposed to handle parameter uncertainties [6], while robust control methodologies address bounded disturbances [7]. Backstepping control, owing to its systematic design framework for strict-feedback nonlinear systems, has been extensively employed in FJR control [8]. However, the traditional backstepping approach suffers from the "complexity explosion" problem—the repeated analytical differentiation of virtual control laws leads to prohibitive computational complexity as the system order increases [9].

To mitigate this issue, dynamic surface control (DSC) and command-filtered control have been introduced. By passing virtual control signals through first-order filters, the analytical differentiation of complex functions is circumvented [10]. Recent advances have incorporated error compensation mechanisms to reduce filtering errors and enhance tracking accuracy [11]. For instance, Hong *et al.* [12] developed a nonsingular fixed-time command-filtered backstepping controller for free-flying flexible-joint space robots, integrating fast fixed-time extended state observers for disturbance estimation. Zhang *et al.* [13] employed continuous sliding mode control with generalized proportional integral observers for FJRs subject to multi-source disturbances. A novel neuro-adaptive command-filtered output-feedback backstepping control scheme was recently proposed for

FJRs [14], which represents a significant advancement in simultaneously addressing input saturation, system uncertainties, and output-feedback constraints.

The challenges of input saturation in FJRs have been addressed through various anti-windup strategies. The mean value theorem combined with hyperbolic tangent functions has been widely used to approximate saturation nonlinearities [15]. Liu *et al.* [16] proposed a model-free adaptive robust control based on time-delay estimation, employing auxiliary systems and adaptive laws based on saturation deviation boundaries to compensate for input saturation effects. Li *et al.* [17] developed a dynamic event-triggered model-free adaptive control approach for robotic manipulators with input saturation, utilizing only input–output data without requiring accurate system dynamics.

Intelligent control methodologies, including neural networks (NNs) and fuzzy logic systems (FLSs), have been extensively investigated for model-free control of uncertain robotic systems [18]. As universal approximators based on the Stone–Weierstrass theorem, these approaches can approximate unknown nonlinear functions with arbitrary accuracy [19]. However, NN and FLS implementations face inherent limitations: the network architecture (layers, nodes, activation functions) and the fuzzy parameters (membership-function centers, widths, and rule weights) require careful selection, and the numerous tuning parameters impose a considerable computational burden [20]. Moreover, the convergence properties of these approaches are often sensitive to initial parameter choices, complicating practical implementation.

Function Approximation Techniques (FAT) have emerged as an alternative paradigm, offering simpler structures and requiring fewer tuning parameters [21]. FAT-based controllers employ orthogonal basis functions—such as Fourier series, Legendre polynomials, or Chebyshev polynomials—to represent unknown time-varying uncertainties as linear combinations of known basis functions with unknown constant coefficients [22]. Izadbaksh and colleagues have extensively explored FAT applications in robot control, demonstrating robust adaptive impedance control using Fourier series and Legendre polynomials [23]. Recent developments have introduced q-analogues of Bernstein-type operators for robot control applications [24], with the q-Bernstein-Schurer operators demonstrating superior approximation capabilities in adaptive control frameworks [25]. Despite these valuable contributions, several critical challenges remain unresolved in FJR control: (1) the simultaneous handling of system uncertainties, input saturation, and complexity explosion; (2) the computational overhead of neuro-fuzzy approaches; (3) the reliance on precise system models or extensive tuning parameters; and (4) the need for improved approximation accuracy with reduced computational burden [14].

Inspired by the preceding discussions, this paper presents a novel model-free control framework for uncertain flexible-joint robots with actuator saturation, leveraging the Bernstein–Schurer–Stancu (BSS) operator as a universal approximator. The BSS operator, a sophisticated generalization of classical Bernstein polynomials incorporating both Schurer's extension for wider domains and Stancu's shifting parameters for enhanced flexibility [26], offers superior approximation properties in various functional spaces [27]. Recent theoretical advances in Stancu-type operators with shape parameters have demonstrated their exceptional convergence characteristics and approximation capabilities for continuous functions [28]. The key contributions of this work are as follows:

- A robust adaptive controller, which operates without requiring precise knowledge of system dynamics, is developed for flexible-joint robots and employs the Bernstein–Schurer–Stancu operator to approximate the combined effects of unknown dynamics, external disturbances, and saturation nonlinearities. This represents the first application of the BSS operator as a universal approximator in the backstepping-based control of flexible-joint robots.
- The complexity explosion issue is systematically addressed through a command-filtered control framework, augmented with error compensation mechanisms that reduce filtering errors and improve tracking accuracy. This integrated approach ensures practical implementability while maintaining theoretical rigor.
- A simple auxiliary system is designed to handle actuator saturation, with its states directly incorporated into the compensated error surfaces that govern the adaptation laws. This approach provides a unified framework for simultaneous uncertainty approximation and saturation compensation.
- Compared to conventional neuro-fuzzy approaches with numerous tuning parameters, the proposed BSS operator requires only the polynomial coefficients to be updated online, significantly reducing the computational burden while maintaining superior approximation capability. This is particularly advantageous for real-time control applications.

The rest of this paper is as follows. Section 2 presents the problem formulation. Section 3 details the command-filtered backstepping control design, along with the adaptive laws for the BSS operator coefficients. Section 4 presents comparative simulation results that demonstrate the effectiveness of the proposed approach. Finally, Section 5 concludes the paper with a summary of the main findings and directions for future research.

II Problem Formulation

A Electrically-driven FJR dynamics

The structure of a flexible-joint robot equipped with actuator dynamics is modeled as

$$D(q)\ddot{q} + C(q,\dot{q})\dot{q} + G(q) + F(\dot{q}) + Kq = rKq_m \quad (1)$$

$$J\ddot{q}_m + B\dot{q}_m + rK(rq_m - q) = u \quad (2)$$

where $q, \dot{q} \in \mathbb{R}^n$ and $\ddot{q} \in \mathbb{R}^n$ are the joint position vector, the vector of joint velocity and the joint acceleration vector, respectively. $q_m, \dot{q}_m \in \mathbb{R}^n$ stand for angular positions and velocities of motor. $D(q) \in \mathbb{R}^{n\times n}$, $C(q,\dot{q}) \in \mathbb{R}^n$ and $G(q) \in \mathbb{R}^n$ are the inertia matrix, Coriolis and centrifugal torques and the vector of gravitational torques, respectively. $J \in \mathbb{R}^{n\times n}$ is the inertia of the motor, $B \in \mathbb{R}^{n\times n}$ is the motor damping and $r \in \mathbb{R}^{n\times n}$ is the reduction gear. $K_m \in \mathbb{R}^{n\times n}$ is the torque constant. Also, u is the torque input at each actuator.

Defining the state vector as $X = [q, \dot{q}, q_m, \dot{q}_m]^T$, the state-space model is expressed as

$$\begin{cases} \dot{x}_1 = x_2 \\ \dot{x}_2 = D^{-1}(x_1)(rKx_3 - Y) \\ \dot{x}_3 = x_4 \\ \dot{x}_4 = J^{-1}(u - Bx_4 - rK(x_3 - x_1)) \end{cases} \tag{3}$$

where $Y = C(x_1, x_2) + G(x_1) + F(x_2) + Kx_1$. Considering motor saturation and external disturbances $d_i(t)$, (3) can be rewritten as

$$\begin{cases} \dot{x}_1 = x_2 \\ \dot{x}_2 = f_1 + x_3 \\ \dot{x}_3 = x_4 \\ \dot{x}_4 = f_2 + \mathrm{sat}(u) \end{cases} \tag{4}$$

in which f_1 and f_2 denote $-D^{-1}(x_1)Y + (D^{-1}(x_1)rK - I_{n\times n})x_3 + d_1(t)$ and $-J^{-1}(Bx_4 + rK(rx_3 - x_1)) + d_2(t) + (J^{-1} - I_{n\times n})\mathrm{sat}(u)$, respectively.

B BSS operator

To approximate the unknown term, the q-analogue of the Bernstein–Schurer–Stancu operator is employed [26]. This operator is selected for its linear-in-the-parameters structure and its universal approximation property, which ensures that any continuous function defined on a compact set can be approximated to any desired level of accuracy through an appropriate choice of parameters. Its construction also yields a regressor vector that significantly simplifying the adaptive control design. The operator is defined as

$$S_{(n,p)}^{(\alpha,\beta)}(f;q,x) = \sum_{k=0}^{n+p} f\left(\frac{[k]_q + \alpha}{[n]_q + \beta}\right) b_{n+p,k}^q(x) \tag{5}$$

where $n \in \mathbb{N}$ is the degree of the polynomial approximation; $p \in \mathbb{N}_0$ is a shift parameter that extends the approximation domain; $\alpha, \beta \in \mathbb{R}$ with $0 \le \alpha \le \beta$ are Stancu parameters providing additional flexibility; and $q \in \mathbb{R}^+$ is the q-parameter, with the operator reducing to its classical form when $q = 1$. Furthermore, $[k]_q = \frac{1-q^k}{1-q}$ denotes the q-integer, and $b_{n+p,k}^q(x) = \binom{n+p}{k}_q x^k (1-x)_q^{n+p-k}$ is the q-Bernstein basis polynomial, which constitutes the elements of the regressor vector.

In the adaptive control law, the operator is utilized to approximate the lumped term $f(x)$ as $\hat{f} = \hat{\theta}^T \Phi$, where $\hat{\theta}$ is a vector of time-varying coefficients updated online via the adaptive laws derived from Lyapunov stability analysis. The regressor vector Φ consists of fixed, predefined q-Bernstein basis functions $b_{n+p,k}^q(x)$. The key advantage of this design is that the regressor vector depends solely on the design parameters (n, p, q) and the argument x, which is often chosen as a reference signal or a bounded function rather than the system states. This alleviates the computational burden and circumvents the need for derivative measurements. The universal approximation property guarantees that the approximation error, represented as $\epsilon = \|f(x) - \hat{f}(x)\|$, remains bounded and can be made arbitrarily small through appropriate selection of n and q, which consequently ensures robust stability of the closed-loop system.

C Auxiliary system

To compensate for the detrimental effects of actuator saturation—a common physical constraint in flexible-joint robot systems—an auxiliary system is introduced as

$$\begin{aligned} \dot{\lambda}_i &= \lambda_{i+1} - p_i \lambda_i \\ \dot{\lambda}_n &= \mathrm{sat}(u(t)) - u(t) - p_n \lambda_n \end{aligned} \tag{6}$$

where $\lambda_i \in \mathbb{R}^n$, for $i = 1, \ldots, n$, are the states of the auxiliary system, $p_i > 0$, for $i = 1, \ldots, n$, are positive design parameters determining the convergence rate of the compensation signals, and n denotes the number of subsystems in the backstepping design.

III Control Design And Stability Analysis

Within the framework of the backstepping method, the proposed controller is developed in four steps, corresponding to the four subsystems described in (4). The BSS operator is employed to approximate the unknown functions f_1 and f_2 in the second and fourth subsystems, respectively.

A Step 1

The tracking error for the first subsystem is defined as

$$\omega_{1i} = x_{1i} - x_{1di} - \lambda_{1i} \tag{7}$$

where x_{1di} is the desired trajectory and λ_{1i} is the state of the auxiliary system introduced to handle input saturation. The virtual control x_{2i}^d is chosen as

$$x_{2i}^d = -k_{1i}\omega_{1i} + \dot{x}_{1di} - p_{1i}\lambda_{1i} \tag{8}$$

where $k_{1i} > 0$ and $p_{1i} > 0$ are design parameters. To reduce the complexity explosion inherent in the backstepping method, the virtual control x_{2i}^d is passed through a first-order filter

$$\alpha_{2i}\dot{x}_{2i}^c + x_{2i}^c = x_{2i}^d \tag{9}$$

where $\alpha_{2i} > 0$ is the filter time constant and x_{2i}^c is the filtered signal. The error surface for the second subsystem is defined as $\omega_{2i} = x_{2i} - x^c_{2i} - \lambda_{2i}$. The derivative of ω_{1i} can be expressed as

$$\dot{\omega}_{1i} = -k_{1i}\omega_{1i} + \omega_{2i} + (x^c_{2i} - x^d_{2i}) \quad (10)$$

To eliminate the effect of the filtered signal error, the compensating signal z_{1i} is designed as

$$\dot{z}_{1i} = -k_{1i}z_{1i} + z_{2i} + (x^c_{2i} - x^d_{2i}) \quad (11)$$

The compensated tracking error signals are defined as

$$\nu_{1i} = \omega_{1i} - z_{1i}, \quad \nu_{2i} = \omega_{2i} - z_{2i} \quad (12)$$

The Lyapunov function candidate in this step is as

$$V_1 = \frac{1}{2}\sum_{i=1}^{n} \nu^2_{1i} \quad (13)$$

Taking the time derivative of V_1 yields

$$\dot{V}_1 = -\sum_{i=1}^{n} k_{1i}\nu^2_{1i} + \sum_{i=1}^{n} \nu_{1i}\nu_{2i} \quad (14)$$

B Step 2

The derivative of the tracking error for the second subsystem is expressed as

$$\dot{\omega}_{2i} = \dot{x}_{2i} - \dot{x}^c_{2i} - \dot{\lambda}_{2i} \quad (15)$$

From the system dynamics (4), we have

$$\dot{x}_{2i} = f_{1i} + x_{3i} \quad (16)$$

Using the BSS operator, the unknown function f_{1i} is approximated as

$$f_{1i} = \Theta^{*T}_{1i}\Phi_{1i} + \epsilon_{1i} \quad (17)$$

where Θ^*_{1i} is the optimal parameter vector, Φ_{1i} is the regressor vector, and ϵ_{1i} is the approximation error bounded by $|\epsilon_{1i}| \le \epsilon^*_{1i}$. The virtual control is proposed as

$$x^d_{3i} = -\hat{\Theta}^T_{1i}\Phi_{1i} - k_{2i}\omega_{2i} - \omega_{1i} + \dot{x}^c_{2i} - p_{2i}\lambda_{2i} \quad (18)$$

where $\hat{\Theta}_{1i}$ is the estimate of Θ^*_{1i} and $k_{2i}, p_{2i} > 0$. The virtual control x^d_{3i} is passed through a first-order filter:

$$\alpha_{3i}\dot{x}^c_{3i} + x^c_{3i} = x^d_{3i} \quad (19)$$

The error surface for the third subsystem is defined as $\omega_{3i} = x_{3i} - x^c_{3i} - \lambda_{3i}$. The derivative of ω_{2i} can be rewritten as

$$\dot{\omega}_{2i} = \tilde{\Theta}^T_{1i}\Phi_{1i} + \epsilon_{1i} + \omega_{3i} - k_{2i}\omega_{2i} - \omega_{1i} + (x^c_{3i} - x^d_{3i}) \quad (20)$$

where $\tilde{\Theta}_{1i} = \hat{\Theta}_{1i} - \Theta^*_{1i}$ is the parameter estimation error. The compensating signal z_{2i} is designed as

$$\dot{z}_{2i} = -k_{2i}z_{2i} - z_{1i} + z_{3i} + (x^c_{3i} - x^d_{3i}) \quad (21)$$

The derivative of the compensated tracking error ν_{2i} is obtained as

$$\dot{\nu}_{2i} = \tilde{\Theta}^T_{1i}\Phi_{1i} + \epsilon_{1i} + \nu_{3i} - \nu_{1i} - k_{2i}\nu_{2i} \quad (22)$$

The Lyapunov function candidate for the second step is chosen as

$$V_2 = V_1 + \frac{1}{2}\sum_{i=1}^{n} \nu^2_{2i} + \frac{1}{2}\sum_{i=1}^{n} \tilde{\Theta}^T_{1i}\gamma^{-1}_{1i}\tilde{\Theta}_{1i} \quad (23)$$

where $\gamma_{1i} > 0$ is the adaptation gain matrix.

The time derivative of V_2 is

$$\begin{aligned}\dot{V}_2 = &-\sum_{i=1}^{n} k_{1i}\nu^2_{1i} - \sum_{i=1}^{n} k_{2i}\nu^2_{2i} + \sum_{i=1}^{n} \nu_{2i}\nu_{3i} \\ &+ \sum_{i=1}^{n} \tilde{\Theta}^T_{1i}(\nu_{2i}\Phi_{1i} - \gamma^{-1}_{1i}\dot{\hat{\Theta}}_{1i}) + \sum_{i=1}^{n} \nu_{2i}\epsilon_{1i}\end{aligned} \quad (24)$$

The adaptation law is chosen as

$$\dot{\hat{\Theta}}_{1i} = \gamma_{1i}(\nu_{2i}\Phi_{1i} - \delta_{1i}\hat{\Theta}_{1i}) \quad (25)$$

where $\delta_{1i} > 0$ is a small design parameter. Using the Young's inequality

$$\nu_{2i}\epsilon_{1i} \le \frac{1}{2}\nu^2_{2i} + \frac{1}{2}\epsilon^{*2}_{1i} \quad (26)$$

$$-\delta_{1i}\tilde{\Theta}^T_{1i}\hat{\Theta}_{1i} \le -\frac{\delta_{1i}}{2}\tilde{\Theta}^T_{1i}\tilde{\Theta}_{1i} + \frac{\delta_{1i}}{2}\|\Theta^*_{1i}\|^2 \quad (27)$$

Thus, $\dot{V}_2$ can be bounded as

$$\begin{aligned}\dot{V}_2 \le &-\sum_{i=1}^{n} k_{1i}\nu^2_{1i} - \sum_{i=1}^{n}(k_{2i} - \frac{1}{2})\nu^2_{2i} + \sum_{i=1}^{n} \nu_{2i}\nu_{3i} \\ &- \sum_{i=1}^{n} \frac{\delta_{1i}}{2}\tilde{\Theta}^T_{1i}\tilde{\Theta}_{1i} + \sum_{i=1}^{n}\left(\frac{\delta_{1i}}{2}\|\Theta^*_{1i}\|^2 + \frac{1}{2}\epsilon^{*2}_{1i}\right)\end{aligned} \quad (28)$$

C Step 3

The tracking error for the third subsystem is defined as

$$\omega_{3i} = x_{3i} - x^c_{3i} - \lambda_{3i} \quad (29)$$

The virtual control x^d_{4i} is chosen as

$$x^d_{4i} = -k_{3i}\omega_{3i} - \omega_{2i} + \dot{x}^c_{3i} - p_{3i}\lambda_{3i} \quad (30)$$

where $k_{3i} > 0$ and $p_{3i} > 0$. The virtual control x^d_{4i} is passed through a first-order filter

$$\alpha_{4i}\dot{x}^c_{4i} + x^c_{4i} = x^d_{4i} \quad (31)$$

The error surface for the fourth subsystem is defined as $\omega_{4i} = x_{4i} - x^c_{4i} - \lambda_{4i}$. The derivative of ω_{3i} is

$$\dot{\omega}_{3i} = -k_{3i}\omega_{3i} + \omega_{4i} - \omega_{2i} + (x^c_{4i} - x^d_{4i}) \quad (32)$$

The compensating signal z_{3i} is designed as

$$\dot{z}_{3i} = -k_{3i}z_{3i} + z_{4i} - z_{2i} + (x^c_{4i} - x^d_{4i}) \quad (33)$$

The derivative of the compensated tracking error $\nu_{3i} = \omega_{3i} - z_{3i}$ is obtained as

$$\dot{\nu}_{3i} = -k_{3i}\nu_{3i} + \nu_{4i} - \nu_{2i} \tag{34}$$

The Lyapunov function candidate for the third step is

$$V_3 = V_2 + \frac{1}{2}\sum_{i=1}^{n}\nu_{3i}^2 \tag{35}$$

The time derivative of V_3 is

$$\begin{aligned}\dot{V}_3 \leq &-\sum_{i=1}^{n}k_{1i}\nu_{1i}^2 - \sum_{i=1}^{n}(k_{2i}-\frac{1}{2})\nu_{2i}^2 - \sum_{i=1}^{n}k_{3i}\nu_{3i}^2 \\ &+\sum_{i=1}^{n}\nu_{3i}\nu_{4i} - \sum_{i=1}^{n}\frac{\delta_{1i}}{2}\tilde{\Theta}_{1i}^T\tilde{\Theta}_{1i} \\ &+\sum_{i=1}^{n}\left(\frac{\delta_{1i}}{2}\|\Theta_{1i}^*\|^2 + \frac{1}{2}\epsilon_{1i}^{*2}\right)\end{aligned} \tag{36}$$

D Step 4

The derivative of the tracking error for the fourth subsystem is expressed as

$$\dot{\omega}_{4i} = \dot{x}_{4i} - \dot{x}_{4i}^c - \dot{\lambda}_{4i} \tag{37}$$

From (4), we have

$$\dot{x}_4 = f_2 + \mathrm{sat}(u) \tag{38}$$

Using the BSS operator, the unknown function f_{2i} is approximated as

$$f_{2i} = \Theta_{2i}^{*T}\Phi_{2i} + \epsilon_{2i} \tag{39}$$

where Θ_{2i}^* is the optimal parameter vector, Φ_{2i} is the regressor vector, and ϵ_{2i} is the approximation error bounded by $|\epsilon_{2i}| \leq \epsilon_{2i}^*$. The actual control input is proposed as

$$u_i = -\hat{\Theta}_{2i}^T\Phi_{2i} - k_{4i}\omega_{4i} - \nu_{3i} + \dot{x}_{4i}^c - p_{4i}\lambda_{4i} \tag{40}$$

where $\hat{\Theta}_{2i}$ is the estimate of Θ_{2i}^* and $k_{4i},\ p_{4i} > 0$. Substituting the control law into $\dot{\omega}_{4i}$ yields

$$\dot{\omega}_{4i} = \tilde{\Theta}_{2i}^T\Phi_{2i} + \epsilon_{2i} - k_{4i}\omega_{4i} - \nu_{3i} \tag{41}$$

where $\tilde{\Theta}_{2i} = \hat{\Theta}_{2i} - \Theta_{2i}^*$ is the parameter estimation error. The compensating signal z_{4i} is designed as

$$\dot{z}_{4i} = -k_{4i}z_{4i} - z_{3i} \tag{42}$$

The derivative of the compensated tracking error $\nu_{4i} = \omega_{4i} - z_{4i}$ is obtained as

$$\dot{\nu}_{4i} = \tilde{\Theta}_{2i}^T\Phi_{2i} + \epsilon_{2i} - k_{4i}\nu_{4i} - \nu_{3i} \tag{43}$$

The Lyapunov function candidate for the fourth step is

$$V_4 = V_3 + \frac{1}{2}\sum_{i=1}^{n}\nu_{4i}^2 + \frac{1}{2}\sum_{i=1}^{n}\tilde{\Theta}_{2i}^T\gamma_{2i}^{-1}\tilde{\Theta}_{2i} \tag{44}$$

where $\gamma_{2i} > 0$ is the adaptation gain matrix. The time derivative of V_4 is

$$\dot{V}_4 = \dot{V}_3 + \sum_{i=1}^{n}\nu_{4i}(\tilde{\Theta}_{2i}^T\Phi_{2i} + \epsilon_{2i} - k_{4i}\nu_{4i} - \nu_{3i}) - \sum_{i=1}^{n}\tilde{\Theta}_{2i}^T\gamma_{2i}^{-1}\dot{\hat{\Theta}}_{2i} \tag{45}$$

The adaptation law is chosen as

$$\dot{\hat{\Theta}}_{2i} = \gamma_{2i}(\nu_{4i}\Phi_{2i} - \delta_{2i}\hat{\Theta}_{2i}) \tag{46}$$

where $\delta_{2i} > 0$ is a small design parameter. Using the Young's inequality

$$\nu_{4i}\epsilon_{2i} \leq \frac{1}{2}\nu_{4i}^2 + \frac{1}{2}\epsilon_{2i}^{*2} \tag{47}$$

$$-\delta_{2i}\tilde{\Theta}_{2i}^T\hat{\Theta}_{2i} \leq -\frac{\delta_{2i}}{2}\tilde{\Theta}_{2i}^T\tilde{\Theta}_{2i} + \frac{\delta_{2i}}{2}\|\Theta_{2i}^*\|^2 \tag{48}$$

Thus, $\dot{V}_4$ can be bounded as

$$\begin{aligned}\dot{V}_4 \leq &-\sum_{i=1}^{n}k_{1i}\nu_{1i}^2 - \sum_{i=1}^{n}(k_{2i}-\frac{1}{2})\nu_{2i}^2 - \sum_{i=1}^{n}k_{3i}\nu_{3i}^2 \\ &-\sum_{i=1}^{n}(k_{4i}-\frac{1}{2})\nu_{4i}^2 - \sum_{i=1}^{n}\frac{\delta_{1i}}{2}\tilde{\Theta}_{1i}^T\tilde{\Theta}_{1i} - \sum_{i=1}^{n}\frac{\delta_{2i}}{2}\tilde{\Theta}_{2i}^T\tilde{\Theta}_{2i} \\ &+\sum_{i=1}^{n}\left(\frac{\delta_{1i}}{2}\|\Theta_{1i}^*\|^2 + \frac{\delta_{2i}}{2}\|\Theta_{2i}^*\|^2 + \frac{1}{2}\epsilon_{1i}^{*2} + \frac{1}{2}\epsilon_{2i}^{*2}\right)\end{aligned} \tag{49}$$

E Theorem

Theorem: For the uncertain flexible-joint robot system subject to actuator saturation (4), the control law (40), together with the adaptation laws (25) and (46), guarantees that all closed-loop signals are uniformly ultimately bounded and that the tracking errors ν_{1i} converge to a small neighborhood around zero.

Proof: From (49), we can write:

$$\dot{V}_4 \leq -\mu V_4 + \rho \tag{50}$$

where

$$\mu = \min\{2k_{1i}, 2(k_{2i}-\frac{1}{2}), 2k_{3i}, 2(k_{4i}-\frac{1}{2}), \delta_{1i}\gamma_{1i}, \delta_{2i}\gamma_{2i}\} \tag{51}$$

$$\rho = \sum_{i=1}^{n}\left(\frac{\delta_{1i}}{2}\|\Theta_{1i}^*\|^2 + \frac{\delta_{2i}}{2}\|\Theta_{2i}^*\|^2 + \frac{1}{2}\epsilon_{1i}^{*2} + \frac{1}{2}\epsilon_{2i}^{*2}\right) \tag{52}$$

Solving the differential inequality yields

$$0 \leq V_4(t) \leq \frac{\rho}{\mu} + (V_4(0) - \frac{\rho}{\mu})e^{-\mu t} \tag{53}$$

Therefore, $V_4(t)$ is bounded for all $t \geq 0$. Consequently, the compensated tracking errors $\nu_{1i}, \nu_{2i}, \nu_{3i}, \nu_{4i}$ and the parameter estimation errors $\tilde{\Theta}_{1i}, \tilde{\Theta}_{2i}$ are uniformly ultimately bounded. Moreover, as $t \longrightarrow \infty$

$$\|\nu_{1i}\| \leq \sqrt{\frac{2\rho}{\mu}} \tag{54}$$

which implies that the tracking error ν_{1i} converges to a small neighborhood of the origin. The size of the residual set can be made arbitrarily small by increasing the control gains k_{ji}, decreasing the approximation errors ϵ_{ji} through an appropriate selection of n, p, and q, or reducing the parameter update gains δ_{ji}.

Remark 1: We recommend the following guidelines for tuning the key design parameters. The control gains k_{ji} determine the convergence rate of the compensated tracking errors; larger values yield faster convergence and smaller ultimate bounds, but excessively high gains may excite unmodeled dynamics or amplify noise. The auxiliary system gains p_{ji} control the convergence rate of the compensation signals. They are recommended to be slightly larger than the corresponding control gains k_{ji} to ensure faster compensation dynamics. The adaptation gains γ_{ji} determine the learning rate of the BSS coefficients. The δ_{ji} modification parameters provide parameter robustness without significantly degrading steady-state accuracy. Finally, for the BSS operator, the polynomial degree $n \in [3, 8]$ and shift parameter $p \in [1, 3]$ offer a practical trade-off between approximation accuracy and computational complexity.

IV Simulation Results

The simulation study is designed in terms of tracking accuracy, computational efficiency, and robustness against uncertainties and input saturation. The two link flexible-joint robot system considered in this study comprises two flexible joints, each driven by a DC motor with actuator dynamics; the system parameters are taken from [15]. The actuator saturation limits are set to $\pm 50\,\mathrm{N}\cdot\mathrm{m}$ for each joint, reflecting practical physical constraints. The desired reference trajectories for the two joints are specified as $q_{1d}(t) = 0.8\sin(0.8t) + 0.3\cos(0.4t)$ rad and $q_{2d}(t) = 0.6\cos(0.6t) + 0.2\sin(0.3t)$ rad, representing time-varying motions that demand precise tracking performance. External disturbances are introduced as $d_1(t) = 0.5\sin(2t)$ and $d_2(t) = 0.4\cos(1.5t)\,\mathrm{N}\cdot\mathrm{m}$ to evaluate the robustness of the proposed controller against exogenous perturbations.

For the BSS operator implementation, the design parameters are selected as follows: polynomial degree $n = 5$, shift parameter $p = 2$, Stancu parameters $\alpha = 0.5$ and $\beta = 1.0$, and the q-parameter $q = 0.95$. These values are chosen to achieve a suitable trade-off between approximation accuracy and computational complexity. The control gains are set to $k_{1i} = 15$, $k_{2i} = 20$, $k_{3i} = 18$, and $k_{4i} = 22$, with filter time constants $\alpha_{2i} = \alpha_{3i} = \alpha_{4i} = 0.02$ s. The adaptation gains are $\gamma_{1i} = \gamma_{2i} = 20$, and the damping parameters are $\delta_{1i} = \delta_{2i} = 0.01$. The auxiliary system parameters are set to $p_{1i} = 5$, $p_{2i} = 6$, $p_{3i} = 7$, and $p_{4i} = 8$. The trajectory tracking of the proposed BSS-based controller is illustrated in Figs. 1–4. Figure 1 presents the actual joint positions versus the desired trajectories for both joints. The results demonstrate that the BSS operator-based adaptive controller achieves satisfactory tracking accuracy, with the actual trajectories nearly coinciding with the reference trajectories throughout the simulation horizon. The control signals shown in Fig. 2 remain well within the specified saturation limits, confirming the effectiveness of the auxiliary compensation system in mitigating actuator saturation effects. The control inputs exhibit smooth profiles without high-frequency chattering, indicating the practical feasibility of the proposed approach. The evolution of the adaptive parameters for the BSS operator is presented in Figs. 3 and 4. The parameters converge to steady-state values within approximately 5 sec, demonstrating the stability of the adaptation process. Notably, only five parameters per subsystem require online adaptation, resulting in only 10 adaptive parameters for the entire system. This minimal parameter count underscores the computational efficiency of the proposed BSS-based approach compared to neuro-fuzzy alternatives. To highlight the advantages of the proposed BSS operator-based approach, Figs. 5–8 present the simulation results obtained using a conventional fuzzy logic controller under identical operating conditions and initial settings. Fig. 5 illustrates the tracking performance achieved by the fuzzy estimator. While the fuzzy controller maintains reasonable tracking performance, it exhibits notable tracking errors, particularly during periods of rapid reference trajectory changes. The corresponding control signals in Fig. 6 exhibit higher amplitudes and more oscillatory behavior compared with the BSS-based control signals, suggesting increased control effort and potential actuator wear.

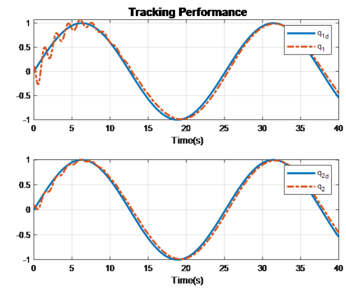

Figure 1. Tracking performance of the proposed BSS operator-based controller: desired trajectories (dashed) and actual joint positions (solid) for joints 1 and 2.

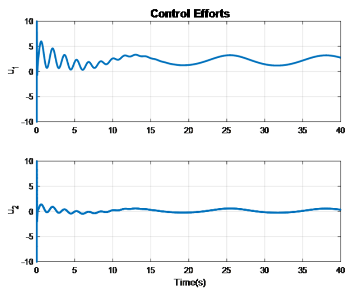

Figure 2. Control input signals generated by the proposed BSS operator-based controller for joints 1 and 2.

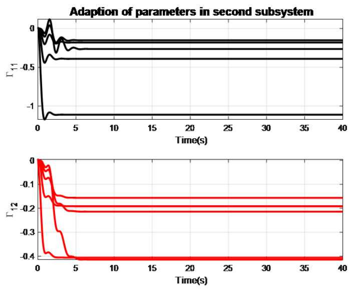

Figure 3. Evolution of the BSS operator adaptive parameters for the second subsystem.

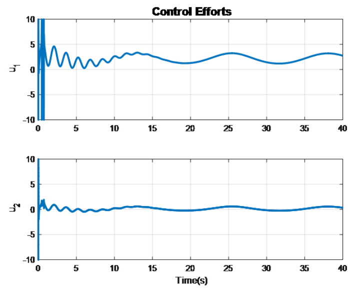

Figure 6. Control input signals generated by the fuzzy logic-based controller for joints 1 and 2.

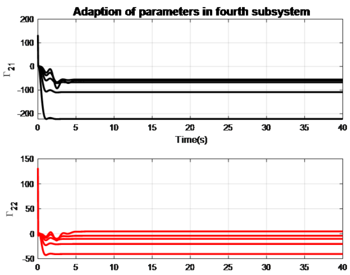

Figure 4. Evolution of the BSS operator adaptive parameters for the fourth subsystem.

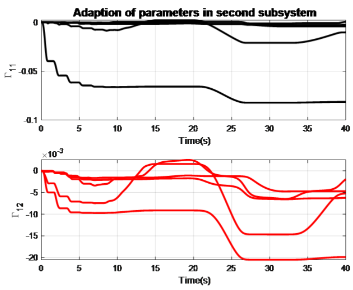

Figure 7. Norm of the adaptive parameter vector for the fuzzy estimator (second subsystem).

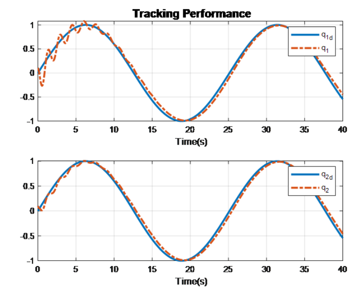

Figure 5. Tracking performance of the fuzzy logic-based controller: desired trajectories (dashed) and actual joint positions (solid) for joints 1 and 2.

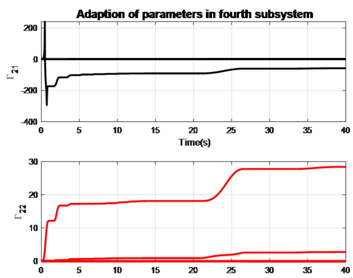

Figure 8. Norm of the adaptive parameter vector for the fuzzy estimator (fourth subsystem).

The adaptive parameters for the fuzzy estimator are depicted in Figs. 7 and 8, which show the norm of the adaptive parameter vectors for the two fuzzy subsystems, providing a compact visualization of the overall adaptation dynamics. While the fuzzy controller requires 49 parameters per subsystem (7 membership functions $\times$ 7 input combinations) to approximate the unknown functions—totaling 98 parameters for the two-joint system—the figures display the aggregated norm values for clarity. The norm trajectories exhibit notable fluctuations and slower convergence rates, indicating the fuzzy controller's sensitivity to system uncertainties and disturbances. In summary, the simulation study provides compelling evidence of the practical viability and superiority of the proposed BSS operator-based, model-free adaptive control framework for uncertain saturated flexible-joint robots.

V Conclusion And Future Work

In this paper, a novel model-free adaptive control scheme has been developed for uncertain flexible-joint robots subject to input saturation, utilizing the q-analogue of the Bernstein–Schurer–Stancu operator as a universal approximator. The command-filtered backstepping approach has been employed to address the complexity explosion problem. To handle actuator saturation, an auxiliary system has been introduced, and its states have been integrated into the compensated error surfaces. The adaptive laws for updating the operator's coefficients have been rigorously derived from Lyapunov stability analysis, ensuring the uniform ultimate boundedness of all closed-loop signals. Comparative simulation results demonstrate that the proposed Bernstein–Schurer–Stancu operator-based controller achieves superior tracking performance over conventional fuzzy controllers, with significantly reduced computational complexity. Future research directions include the integration of reinforcement learning techniques to enable optimal adaptive parameter tuning and further enhance the self-learning capabilities of the proposed control framework in uncertain environments.

References

[1] Pan, C., *et al.* Neuro-adaptive command-filtered backstepping control of uncertain flexible-joint manipulators with input saturation via output feedback, *Scientific Reports*, vol. 15, Art. no. 17254, 2025.

[2] Xie, S., Sun, W., Su, S.F. Adaptive performance optimal control for flexible-joint robots with random noises: Design and experiment, *Applied Mathematical Modelling*, vol. 138, Art. no. 115741, 2025.

[3] Ngo, V.T., Liu, Y.C. On tracking control of robot manipulator with flexible joints in operational space, *IFAC-PapersOnLine*, vol. 56, no. 2, pp. 1307-1312, 2023.

[4] Li, X., *et al.* Identification and control of flexible joint robots based on a composite-learning optimal bounded ellipsoid algorithm and prescribe performance control technique, *Applied Sciences*, vol. 14, no. 10, Art. no. 4030, 2024.

[5] Z. Wang and T. Zhang, Adaptive fixed-time prescribed performance control of flexible-joint manipulator with unmodeled dynamics and dead-zone, *Asian Journal of Control*, vol. 27, no. 6, pp. 3016-3030, 2025.

[6] Yuan, J., Sun, W. Adaptive fuzzy tracking control for multiple-input multiple-output nonlinear systems with sensor faults and experiment in the flexible-joint robot, *Asian Journal of Control*, vol. 27, pp. 470-487, 2025.

[7] Zhang, Y., Sun, R., Shang, J. Prescribed performance bounded-H_∞ control for flexible-joint manipulators without initial condition restriction, *Sensors*, vol. 25, no. 7, Art. no. 2195, 2025.

[8] Xu, B. Composite learning control of flexible-link manipulator using NN and DOB, *IEEE Transactions on Systems, Man, and Cybernetics: Systems*, vol. 48, no. 11, pp. 1979-1985, 2018.

[9] Esmaeili, N., Alfi, A., Khosravi, H. Balancing and trajectory tracking of two-wheeled mobile robot using backstepping sliding mode control: design and experiments, *Journal of Intelligent & Robotic Systems*, vol. 87, no. 3, pp. 601-613, 2017.

[10] Keighobadi, J., Mehrjouyan, A., Alfi, A. Efficient learning control of uncertain nonlinear systems with input constraints: A disturbance observer-based neural network approach, *International Journal of Dynamics and Control*, vol. 12, pp. 3392-3406, 2024.

[11] Keighobadi, J., *et al.* Composite fuzzy voltage-based command-filtered learning control of electrically-driven robots with input delay using disturbance observer, *Journal of the Franklin Institute*, vol. 360, no. 2, pp. 813-840, 2023.

[12] Li, T., Li, S. Fixed-time adaptive dynamic event-triggered control of flexible-joint robots with prescribed performance and time delays, *ISA Transactions*, vol. 140, pp. 198-223, 2023.

[13] Zhang, Y., *et al.* Robust command-filtered control with prescribed performance for flexible-joint robots, *IEEE Transactions on Instrumentation and Measurement*, vol. 72, pp. 1-13, 2023.

[14] Pan, C., *et al.* Neuro-adaptive command-filtered backstepping control of uncertain flexible-joint manipulators with input saturation via output feedback, *Scientific Reports*, vol. 15, Art. no. 17254, 2025.

[15] Arefi, M.M., *et al.* Command filtered backstepping control of constrained flexible joint robotic manipulator, *IET Control Theory & Applications*, vol. 17, no. 18, pp. 2506-2518, 2023.

[16] Liu, X., Wang, L., Yang, Y. Model-free adaptive robust control based on TDE for robot with disturbance and input saturation, *Robotica*, 2023.

[17] Li, J., *et al.* Dynamic event-triggered model-free adaptive control for robotic manipulator with input saturation, in: *Proc. 2025 1st International Symposium on E-CARGO and Applications (E-CARGO)*, pp. 74-79, 2025.

[18] Li, X., *et al.* Identification and control of flexible joint robots based on a composite-learning optimal bounded ellipsoid algorithm and prescribe performance control technique, *Applied Sciences*, vol. 14, no. 10, Art. no. 4030, 2024.

[19] Cybenko, G. Approximation by superpositions of a sigmoidal function, *Mathematics of Control, Signals, and Systems*, vol. 2, no. 4, pp. 303-314, 1989.

[20] Yuan, J., Sun, W. Adaptive fuzzy tracking control for multiple-input multiple-output nonlinear systems with sensor faults and experiment in the flexible-joint robot, *Asian Journal of Control*, vol. 27, pp. 470-487, 2025.

[21] Keighobadi, J., *et al.* Compound FAT-based prespecified performance learning control of robotic manipulators with actuator dynamics, *ISA Transactions*, vol. 131, pp. 246-263, 2022.

[22] Deylami, A., Izadbakhsh, A. Observer-based adaptive control of cooperative multiple manipulators using the Mastroianni operators as uncertainty approximator, *International Journal of Robust and Nonlinear Control*, vol. 32, no. 6, pp. 3625-3646, 2022.

[23] Cheng, X., *et al.* Adaptive neural backstepping control for flexible-joint robot manipulator with bounded torque inputs, *Neurocomputing*, vol. 458, pp. 70-86, 2021.

[24] Sidharth, M., Ispir, N., Agrawal, P.N. Approximation of B-continuous and B-differentiable functions by GBS operators of q-Bernstein-Schurer-Stancu type, *Turkish Journal of Mathematics*, vol. 40, pp. 1298-1315, 2016.

[25] Bárbous, D., Muraru, C.V. Approximating B-continuous functions using GBS operators of Bernstein-Schurer-Stancu type based on q-integers, *Applied Mathematics and Computation*, vol. 259, pp. 80-87, 2015.

[26] Alotaibi, A., Nasiruzzaman, M., Mohiuddine, S.A. Approximation properties by Schurer type q-Kantorovich-Stancu shifted knots operators, *Journal of Inequalities and Applications*, vol. 2024, Art. no. 159, 2024.

[27] Nasiruzzaman, M., *et al.* Approximation properties by shifted knots type of α-Bernstein-Kantorovich-Stancu operators, *Journal of Inequalities and Applications*, vol. 2024, Art. no. 85, 2024.

[28] Nasiruzzaman, M. Approximation by Stancu-type α-Bernstein-Schurer-Kantorovich operators, *Journal of Inequalities and Applications*, vol. 2025, Art. no. 48, 2025.